Acc. Chem. Res. **1999,** *32,* 360−367

Unfolding, Refolding, and Hydration of Proteins in the Gas Phase

MARTIN F. JARROLD
Department of Chemistry, Northwestern University, 2145 Sheridan Road, Evanston Illinois 60208

Received May 1, 1998

Introduction

The gas phase is an unusual environment for studies of biomolecules that function in aqueous solution. But the motivation for these studies is to provide a deeper understanding of the intramolecular interactions and hydration interactions that determine the conformations, and ultimately the physiological properties, of these molecules in solution. Studies of unsolvated proteins provide information about their intrinsic intramolecular interactions. This information will facilitate the refinement and testing of the theoretical methods necessary to understand protein conformations and folding processes. Gas-phase studies also offer new opportunities to study hydration interactions. Starting with an unsolvated protein ion in the gas phase, it is possible to hydrate it, one water molecule at a time, and study the hydration process in exquisite detail. $\Delta H°$ and $\Delta S°$ of hydration, as a function of the number of adsorbed water molecules, can be obtained from these studies, along with information about how hydration affects the conformation.

It is not easy to place intact biological molecules into the gas phase. The studies described here were made possible by the recent development of soft desorption and ionization techniques.[1,2] Mass spectrometry is now routinely used to determine the molecular weights of large biomolecules. Methods to obtain sequence information by mass spectrometry have been developed, and mass spectrometry may soon be used to help diagnose diseases and design treatment strategies.[3] However, in addition to these important analytical applications, the development of soft ionization techniques has opened the door to an examination of the properties of unsolvated biomolecules, and several groups have started to examine the structures of gas-phase protein ions. McLafferty and collaborators have used H/D exchange.[4,5] This work revealed the presence of multiple conformations for unsolvated protein ions, and has provided evidence for gas-phase unfolding and refolding processes. However, the interpretation of gas-phase H/D exchange data remains controversial.[6] Douglas, Cooks, and their collaborators have used ion beam scattering to measure collision cross sections for unsolvated proteins and found that the cross section increases with increasing charge.[7,8] Other methods that have been used in an effort to deduce structural information include measurement of the surface defects generated by high-energy impact of protein ions,[9] the modeling of gas-phase basicities,[10] and the analysis of fragment relative kinetic energies.[11] In the work described here we have used ion mobility measurements, the gas-phase analogue of electrophoresis, to probe the conformations.[12−15] The mobility of an ion in the gas phase, how rapidly it moves through a buffer gas under the influence of a weak electric field, depends on the ion's average collision cross section with the buffer gas. A protein in an unfolded conformation has a large collision cross section, and it can easily be resolved from the folded conformation which has a much smaller cross section. Mobility measurements are also being used by Bowers[13] and Clemmer[15] and their collaborators. Bowers' group has focused mainly on studies of small peptides, while Clemmer's is exploring a combinatorial approach to understanding secondary structure.

How Are the Experiments Done?

The experiments were performed using an injected ion drift tube apparatus shown in Figure 1. The apparatus is equipped with an electrospray source that consists of a hypodermic needle, held at around 5 kV, and a plate at near ground potential with a small hole into the vacuum chamber. A protein solution is slowly pumped through the hypodermic needle and nebulized into small charged droplets. The charged droplets evaporate solvent as they travel through air toward the plate, though how the unsolvated ions are produced from these droplets remains controversial. After passing through the aperture into the vacuum chamber, the protein ions enter a heatable desolvation region where any remaining solvent molecules can be removed.

Electrospray ionization produces proteins in a distribution of protonated or deprotonated charge states.[16] Figure 2 shows a positive ion mass spectrum recorded for bovine cytochrome *c*. The peaks in the spectrum are due to different charge states. When an unacidified solution is electrosprayed, the charge state distribution peaks around $(M + 8H)^{8+}$. Higher charge states, up to +20, can be produced by electrospraying acidified solutions. Cytochrome *c* is denatured in acidic solutions, and the increase in the charge is believed to result from the unfolded protein exposing more basic sites.[17] Lower charge states can be produced by adding a base to the desolvation region so that gas-phase proton-transfer reactions lower the charge.[4]

To probe their conformation, ions are focused into a low-energy ion beam, and injected into the drift tube

Martin F. Jarrold was born in England. He obtained his undergraduate and graduate degrees from the University of Warwick. He was a NATO Postdoctoral fellow with Michael T. Bowers at the University of California, Santa Barbara, and a Member of Technical Staff in the Physics Research Division of AT&T Bell Laboratories in Murray Hill, NJ. Since 1992 he has been a Professor of Chemistry at Northwestern University. In addition to his interests in the work described in this Account, his research group is using a variety of experimental techniques to examine the structures and properties of atomic clusters.

10.1021/ar960081x CCC: $18.00
Published on Web 11/13/1998

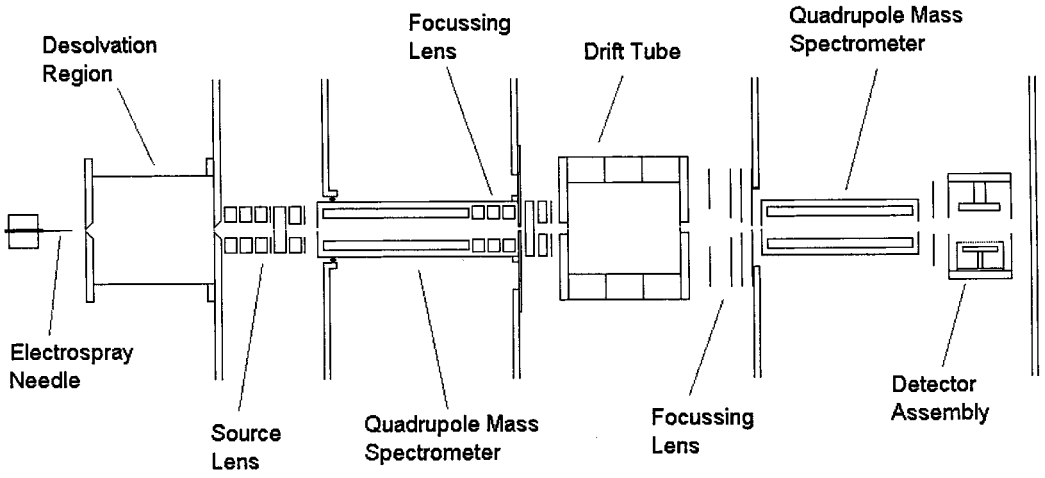

FIGURE 1. Schematic diagram of the experimental apparatus used to study gas-phase proteins.

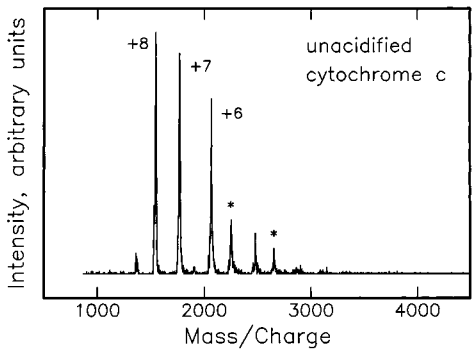

FIGURE 2. Electrospray mass spectrum for an unacidified solution of cytochrome *c*. Peaks due to multimers are marked with an asterisk.

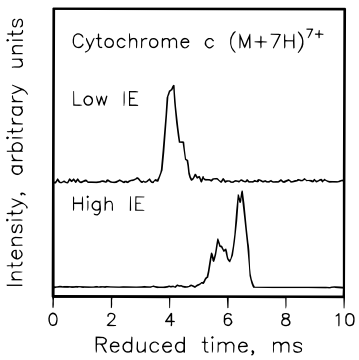

FIGURE 3. Drift time distributions recorded for cytochrome *c* $(M + 7H)^{7+}$ with low (175 eV) and high (2100 eV) injection energies.

through a small aperture. The drift tube contains helium buffer gas at a pressure of a few Torr. At the other side of the drift tube, some of the ions exit through another small aperture, pass through a second quadrupole mass spectrometer, and are then detected. The amount of time the ions spend traveling across the drift tube is determined by injecting 50 μs pulses of ions and recording the arrival time distribution at the detector. The drift time, t_D, is converted into collision cross sections using[18]

$$\Omega_{avg}^{(1,1)} = \frac{(18\pi)^{1/2}}{16}\left[\frac{1}{m_b} + \frac{1}{m}\right]^{1/2}\frac{ze}{(k_B T)^{1/2}}\frac{1}{\rho}\frac{t_D V}{L^2} \qquad (1)$$

where m and m_b are the masses of the ion and buffer gas, ze is the charge, ρ is the buffer gas number density, L is the drift tube length, and V is the voltage across the drift tube.

Cross Section Calculations

The ion mobility measurements are analyzed by calculating cross sections for conformations obtained from molecular dynamics simulations and comparing them to the measured quantities. The cross section in eq 1 above, $\Omega_{avg}^{(1,1)}$, is really a collision integral which should be evaluated by averaging the momentum transfer cross section over the relative velocity distribution and the collision geometry.[18] The momentum transfer cross section depends on the scattering angles between the incoming and outgoing trajectories in collisions between the polyatomic ion and buffer gas atoms. To determine the scattering angle, it is necessary to define a realistic intermolecular potential and perform trajectory calculations.[19] In early studies, the collision integral was approximated by the geometric cross section, but this was found to be inadequate for larger peptides and proteins, where the details of the scattering process must be taken into account. Around 10^5–10^6 trajectories are run to determine an accurate value for the collision integral, so this method requires large amounts of computer time. We have also developed an exact hard spheres scattering model,[20] which treats the scattering between the ion and buffer gas atoms correctly (within the hard sphere limit) but ignores the long-range interactions. Calculations using this model require much less computer time, and for proteins the calculated cross sections are within a few percent of the values determined by the trajectory method.

Ion Mobility Studies of Unsolvated Proteins: Cytochrome *c*

Figure 3 shows drift time distributions measured for the $(M + 7H)^{7+}$ charge state of cytochrome *c*. Results are shown in the figure for two injection energies (the injection energy is the kinetic energy that the ions have

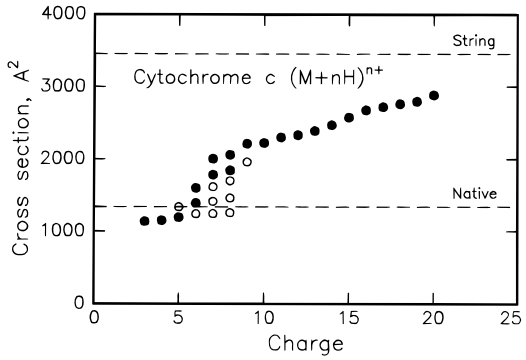

FIGURE 4. Cross sections derived for the main features observed in the drift time distributions of cytochrome *c*. The filled points are for features observed at high injection energies, and the open points are for metastable conformations observed at lower injection energies. The dashed lines show the cross sections calculated for the crystal structure coordinates and for a fully extended string.

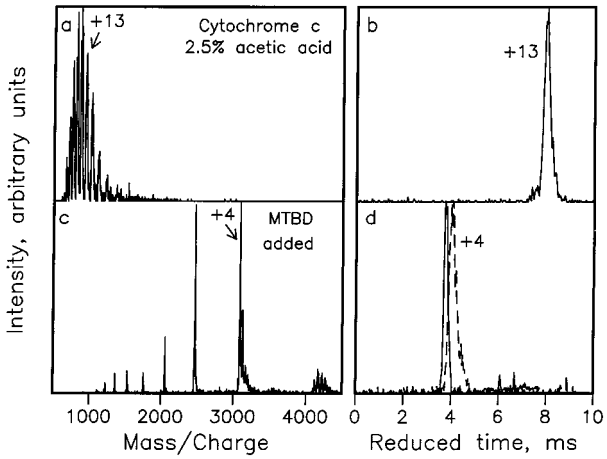

FIGURE 5. Mass spectra and drift time distributions measured for an acidified solution of cytochrome *c* without MTBD added to the desolvation region (top) and with MTDB added to the desolvation region (bottom). The drift time distributions are plotted against a reduced time scale obtained by multiplying the measured time by the charge.

when they enter the drift tube). At high injection energies the ions are heated by collisions with the buffer gas as they enter the drift tube and may undergo conformational changes while they are hot. With a low injection energy, a single broad peak is observed for cytochrome *c* $(M + 7H)^{7+}$, while with a high injection energy there are two incompletely resolved features at significantly longer drift times. A longer drift time indicates a larger collision cross section.

Figure 4 shows the cross sections derived for the main features observed in the drift time distributions of the +3 to +20 charge states of cytochrome *c*.[21] The dashed lines show the cross sections calculated for the native conformation (crystal structure coordinates[22]) and for a fully extended string generated by setting almost all torsion angles to 180°. Crystal structure coordinates and NMR coordinates gave virtually identical cross sections. The filled points show features observed at high injection energies, while the open points show additional features present at lower injection energies. The +3 to +5 charge states have cross sections that are slightly smaller than expected for the native conformation, suggesting that the protein packs more tightly in the absence of the solvent.[23,24] With low injection energies, the +6 and +7 charge states also have cross sections that are close to those expected for the native conformation, but when collisionally heated these charge states unfold and the cross sections increase significantly. For the higher charge states only unfolded conformations are observed. The sharp unfolding transition that occurs with increasing charge is presumably driven by Coulomb repulsion, and it is somewhat analogous to acid denaturation in solution. A similar unfolding transition has been observed for apomyglobin.[25]

The +3 to +5 charge states of cytochrome *c* exist in compact folded conformations even when they are produced by proton transfer from higher charge states that are unfolded.[26] Figure 5(a) shows a mass spectrum measured for an acidified solution of cytochrome *c*. The charge distribution peaks around +14, indicating that the protein is unfolded in solution. The drift time measured for the +13 charge state, Figure 5b, indicates that the protein ions are unfolded in the gas phase. Figure 5c shows the mass spectrum recorded after a strong base (MTBD, 1,3,4,6,7,8-hexahydro-1-methyl-2*H*-pyrimido[1,2-*a*]pyrimidine) was introduced into the desolvation region. Gas-phase proton transfer reactions lower the charge and the distribution peaks at +4. Drift time distributions measured for the +4 charge state are shown in Figure 5d. The dashed line shows the distribution measured at low injection energy, and the solid line is the distribution measured with a high injection energy. The measured drift time is now close to that expected for the native conformation (4.4 ms), indicating that the protein folds in the gas phase after some of the charge is removed. The distribution narrows and shifts to slightly shorter time as the injection energy is raised. This indicates that the protein does not achieve a well-ordered state in the initial collapse from the unfolded conformation. However, with further collisional heating it appears to adopt a more-ordered state. There must be activation barriers that separate the disordered states produced in the initial collapse from the more-ordered state produced after collisional heating. The +6 charge state of apomyoglobin provides an even more striking example of an activation barrier for gas-phase protein folding.[25] It is unlikely that gas-phase folding leads to a conformation similar to the native conformation in solution because there are probably lower energy gas-phase conformations that are more kinetically accessible than the native conformation.

By electrospraying an unacidified solution and operating with a low injection energy, the +7 charge states of cytochrome *c* can be generated in a folded conformation that retains a memory of the structure in solution.[27] Figure 6 shows distributions measured for the folded +7 charge state as a function of the drift tube temperature. The drift time scale has been converted to a collision cross section scale so that distributions measured at different temperatures can easily be compared. As the temperature

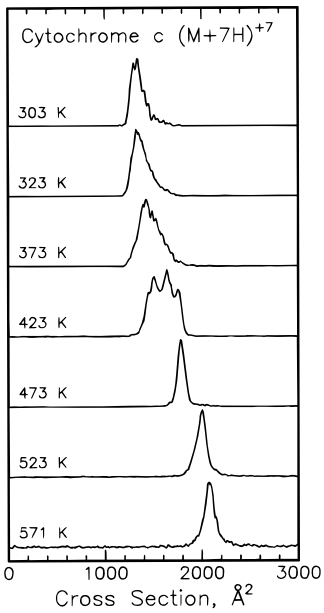

FIGURE 6. Distributions measured for the folded +7 charge state of cytochrome *c* as a function of drift tube temperature. The drift time scale has been converted to a cross section scale.

is raised the protein unfolds. A number of unfolding intermediates can be seen, particularly around 423 K. This unfolding process is analogous to thermal denaturation in solution. The +6 charge state also unfolds as the temperature is raised, but the +5 charge state does not unfold at temperatures up to 570 K, at least within the time scale of our experiments.[28] The ability to put a temperature scale to the conformational changes makes a comparison with molecular dynamics simulations possible.

Molecular Dynamics Simulations of Gas-Phase Proteins

Molecular dynamics (MD) simulations using empirical force fields have been widely used to study biological molecules. The availability of experimental results for unsolvated proteins provides an opportunity to test the simulations without having to worry about the solvent. For the lower charge states of cytochrome *c*, the number of basic residues exceeds the number of protons, and so there are many different ways of arranging the protons among the basic sites (different proton configurations).[29] Since Coulomb repulsion between the protons is significant, the lowest energy proton configuration is probably different for different conformations, and redistribution of the protons may contribute to the activation energies associated with conformational changes.

It is not possible to consider all of the different proton configurations for cytochrome *c* in detail, so we determined the relative energies of all possible configurations for the +5 and +7 charge states in the native conformation and then performed MD simulations using the CHARMM[30] force field for the 10 lowest energy ones for both charge states.[28] At 300 K we performed ten 240 ps simulations for each charge state while at 600 K we performed ten

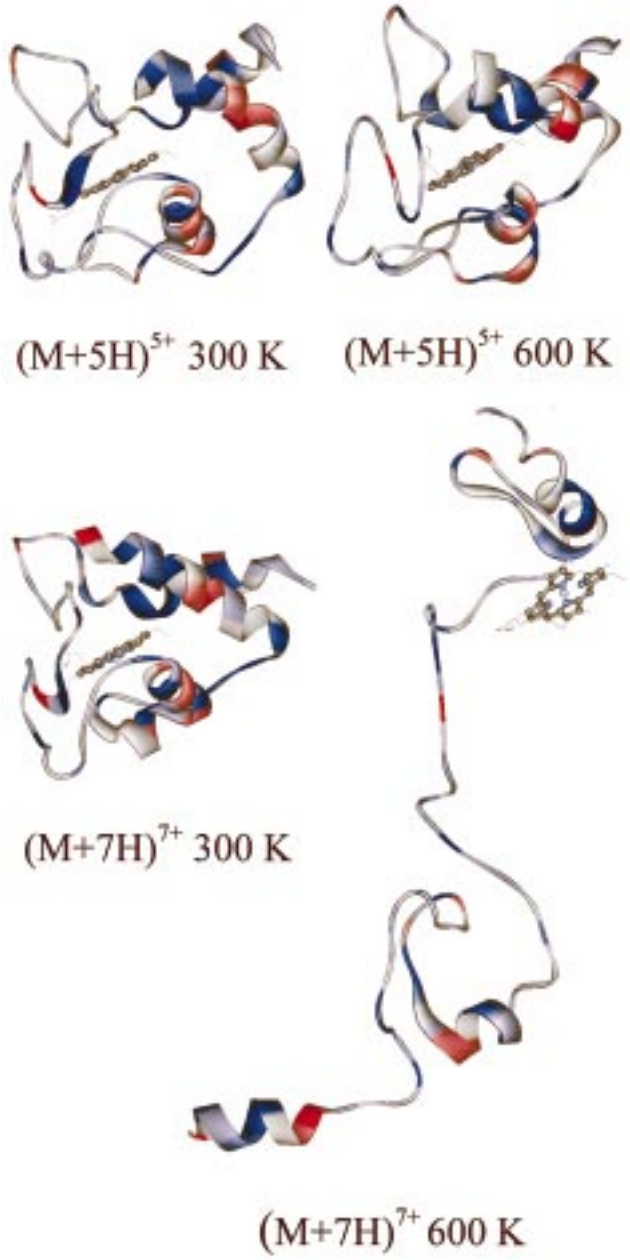

FIGURE 7. Conformations from MD simulations for the +5 and +7 charge states of cytochrome *c* at 300 and 600 K. At 600 K the +7 charge state has unfolded.

480 ps simulations for each charge state. The starting conformation was the crystal structure. All the residues except for the protonated ones were neutral; hence, zwitterions which may exist in solution are assumed to be absent in the gas phase. Figure 7 shows examples of conformations from the MD simulations. In the 300 K simulations, the +5 charge state remains similar to the crystal structure. Essentially all of the secondary structure is retained along with the main features of the tertiary structure. The protonated residues are "self-solvated" by hydrogen bonds to oxygens in backbone carbonyl groups and side chains. This is accomplished without significantly disturbing the overall structure. The simulations for the +7 charge state at 300 K also retain much of the three-dimensional structure of the native conformation,

Table 1. Comparison of the Average Cross Sections Determined from the MD Simulations with the Experimental Values for the +5 and +7 Charge States of Cytochrome *c*

charge state	MD simulations		experiment	
	300 K	600 K	303 K	571 K
+5	1381	1410	1218	1306
+7	1466	1554−2065	1338	2086

though the +7 charge state is further removed from the crystal structure than the +5 charge state.

When the temperature is raised to 600 K, the +5 charge state still remains relatively compact and keeps most of the secondary structure of the native conformation. The terminal helix contact, an important tertiary structure interaction, is retained in all of the +5 simulations. In contrast, at 600 K the +7 charge state unfolds within the first 240 ps, and the terminal helix contact is lost in all of these simulations. The simulations performed for different +7 proton configurations show a wide dispersion in the degree of unfolding, so the location of the protons affects the unfolding trajectory.

The simulations are in qualitative agreement with the experimental observations: the +7 charge state unfolds as the temperature is raised while the +5 charge state remains folded. Average cross sections determined from the simulations are compared with the experimental values in Table 1. For the +7 charge state at 600 K, where different proton configurations show a wide dispersion in the degree of unfolding, the range of average cross sections obtained from the individual simulations is given. The quantitative agreement between the measured and calculated cross sections is relatively poor. Nevertheless, the qualitative agreement is encouraging. The MD simulations were only performed for a fraction of a nanosecond while the experimental time scale is milliseconds. If the simulations were run for much longer, the conformations might move further from the initial (crystal structure) conformation at 300 K and the +7 charge state might unfold further at 600 K. Another significant problem with the simulations is that the protons are not mobile. The protons are assigned to specific basic residues at the start of the simulation and remain fixed. This may hinder the ability of the system to find the lowest energy conformation.

$\Delta H°$ and $\Delta S°$ for the First Few Steps in the Hydration of BPTI

The ability to generate dehydrated proteins in the gas phase provides new opportunities to examine the issue of protein hydration at a microscopic level. There are two basic ways to examine hydrated proteins in the gas phase: either leave water on the protein ion when it is produced or add water to a dehydrated protein. Chait and collaborators[31] and Williams and collaborators[32] have used the first approach. They operated their electrospray sources so that their ions were not completely dehydrated. The other approach to studying protein hydration is to start with a dehydrated protein ion in the gas phase and to rehydrate it by exposing it to water vapor. The number of adsorbed water molecules can be determined by mass spectrometry, and if an equilibrium

$$(M + mH)^{m+}\cdot(H_2O)_n + H_2O \rightleftarrows (M + mH)^{m+}\cdot(H_2O)_{n+1} \quad (2)$$

can be established, equilibrium constants can be determined from the water vapor pressure and the relative intensities of the $(M + mH)^{m+}\cdot(H_2O)_n$ and $(M + mH)^{m+}\cdot(H_2O)_{n+1}$ peaks in the mass spectrum. An equilibrium constant measured at a single temperature provides the free energy change for hydration at that temperature, but if equilibrium constants can be measured as a function of temperature, the enthalpy and entropy changes associated with adsorbing a particular water molecule can be determined. $\Delta H°$ and $\Delta S°$ can be measured as a function of the number of adsorbed water molecules to follow the development of the hydration shell. Previously, thermodynamic information about protein hydration has been obtained from the hydration of protein films.[33] However, the information obtained from these studies is not completely reliable because of hysteresis effects. Furthermore, only average values can be obtained.

The rehydration approach described above was first used by Kebarle and collaborators[34] to measure hydration free energies at 293 K for several small peptides in the gas phase. We have used this approach to measure $\Delta H°$ and $\Delta S°$ for the first few water molecules adsorbed on the $(M + 6H)^{6+}$ charge state of BPTI (bovine pancreatic trypsin inhibitor).[35] BPTI was selected for these studies because it is a small (58 residues), well-characterized protein with three disulfide bridges that partially lock the backbone in place and make BPTI resistant to denaturation. To determine equilibrium constants, water vapor was introduced into the drift tube and mass spectra were measured as a function of the water vapor pressure. Equilibrium constants were measured over a drift tube temperature range from 223 to 273 K. At temperatures above 273 K only a small amount of water adsorbed. $\Delta H°$ and $\Delta S°$ determined from the equilibrium constants for the first few water molecules adsorbed onto BPTI are shown in Figure 8. $\Delta H°$ and $\Delta S°$ for the fourth and fifth water molecules have a large uncertainty because their equilibrium constants were only measured over a narrow temperature range. The solid lines in Figure 8 show $\Delta H°$ and $\Delta S°$ for transferring a water molecule from the gas phase to the liquid.

$\Delta H°$ and $\Delta S°$ for adsorption of the first water molecule onto BPTI are substantially more negative than for subsequent water molecules. The main contribution to the entropy change is expected to come from the translational entropy of the water molecule. Taking into account the translational, rotational, and estimated vibrational contributions, $\Delta S°$ should be between -105 and -145 J K^{-1} mol^{-1}. The measured $\Delta S°$ for the first water molecule, -259 J K^{-1} mol^{-1}, is much more negative. The difference between the measured and estimated $\Delta S°$ cannot be

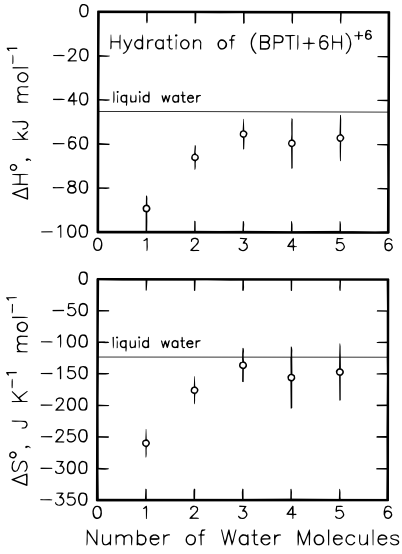

FIGURE 8. $\Delta H°$ and $\Delta S°$ for the adsorption of the first few water molecules on BPTI $(M + 6H)^{6+}$. The solid lines show $\Delta H°$ and $\Delta S°$ for transferring a water molecule from the gas phase to the liquid.

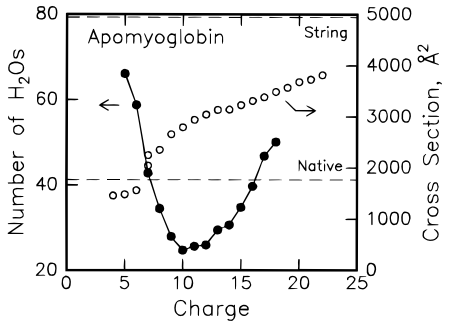

FIGURE 9. Average number of water molecules adsorbed on apomyglobin $(M + mH)^{m+}$ ions with 0.73 Torr of water vapor at 253 K (filled circles and left-hand scale). The average cross sections determined from mobility measurements in helium (open circles and right-hand scale) are also shown. The dashed lines show cross sections calculated for crystal structure coordinates and an extended string.

accounted for by the entropy of the water molecule. Thus, the entropy of the protein must decrease substantially when the first water molecule is adsorbed. This entropy is presumably derived from the remaining configurational entropy of the protein. The loss of configurational entropy probably results from the first water molecule locking different parts of the backbone together. This can occur with structural water molecules. Four structural water molecules have been identified for BPTI. They are conserved in the three crystal structures that have been reported for BPTI,[36] and they have been observed by NMR in solution.[37] One of the structural water molecules is hydrogen bonded in a pocket to Cys38, Cys14, and Thr11. The other three form a hydrogen-bonded cluster that sits in another pocket. The isolated structural water molecule is unusual in that it forms four hydrogen bonds to the protein. Calculations suggest that this is the most strongly bound hydration site on BPTI,[38] with a hydration energy of around 105 kJ mol^{-1}, so this is a good candidate for the adsorption site of the first water molecule, since the first water also has a large enthalpy change (see Figure 8). In the pocket occupied by the isolated structural water molecule, Cys14 and Cys38 are already linked by a disulfide bridge. However, a hydrogen bond to Thr11 will constrain the protein, and Thr11 is hydrogen bonded to Gly36, so introducing a water molecule into this site may cause the protein around the pocket to order.

Saturation Studies and Conformational Changes Induced by Hydration

Saturation studies are performed with a water vapor pressure close to the equilibrium vapor pressure at the temperature of the drift tube.[39] The average number of adsorbed water molecules is determined from mass spectra of the ions exiting the drift tube. Figure 9 shows a plot of the average number of water molecules adsorbed onto apomyglobin $(M + mH)^{m+}$ ions with 0.73 Torr of water vapor and a drift tube temperature of 253 K. Again, the lowered temperature is used to promote rehydration. The average cross sections determined from mobility measurements in helium are also shown in Figure 9. The dashed lines show cross sections calculated for the native conformation and an extended string. Apomyglobin is larger than cytochrome *c*, and the unfolding transition is broader and shifted to slightly higher charge. The average number of water molecules adsorbed by the +5 and +6 charge states of apomyglobin is around 60. The average decreases to around 25 on the $(M + 10H)^{10+}$ ion, and then gradually increases again. The sharp decrease in the amount of adsorbed water is clearly correlated with the unfolding transition. A similar correlation was found with cytochrome *c*.

One would expect the number of water molecules adsorbed by the unfolded conformations to be larger than the number adsorbed by the folded ones. The solvation energies of proteins are usually estimated from an accessible surface area (ASA) model.[40] That the number of water molecules adsorbed by the unfolded charge states is substantially *less* than by the folded ones clearly conflicts with the predictions of this model. This suggests that cooperative effects, where the water molecules interact strongly with more than one site on the protein, are important in the hydration of the folded conformation. When the protein unfolds, the sites are separated and the water can only interact with one of them.

While there is a sharp unfolding transition between the +5 and +7 charge states of cytochrome *c* in the gas phase, in solution charge states up to around +11 remain folded,[41] so if water molecules are added to the unfolded $(M + 7H)^{7+}$ charge state in the gas phase, at some point it should fold. Figure 10 shows drift time distributions recorded for the folded $(M + 5H)^{5+}$ and the unfolded $(M + 7H)^{7+}$ charge states of cytochrome *c* as a function of water vapor pressure. For the folded +5 charge state, the peak remains in approximately the same position as the number of adsorbed water molecules increases. For the unfolded +7 charge state there are two peaks present in the drift time distribution in the absence of the water, and

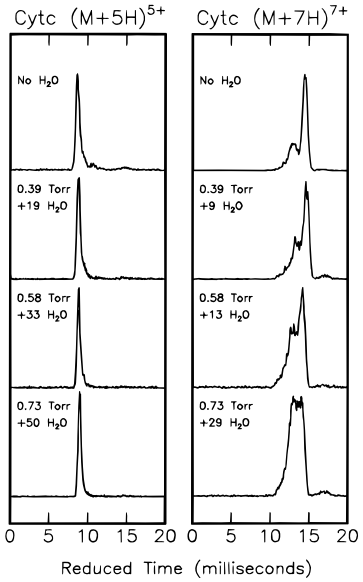

FIGURE 10. Drift time distributions measured for the $(M + 5H)^{5+}$ and $(M + 7H)^{7+}$ charge states of cytochrome *c* with 0.00, 0.39, 0.58, and 0.73 Torr of water vapor at 253 K. The water vapor plus helium buffer gas pressure was around 5.0 Torr. The drift time scale has been approximately corrected for the different water vapor pressures using Blanc's law,[18] and the drift times have been multiplied by the charge. The average numbers of water molecules adsorbed at each water vapor pressure by the two charge states are shown on the plot.

as the number of adsorbed water molecules increases, the distribution shifts over to the more folded conformation at shorter time. The addition of only 29 water molecules is apparently enough to promote the folding of the +7 charge state to a more compact conformation. However, more water molecules are needed to drive the +7 charge state to a completely folded conformation which would be at ~9 ms under the conditions used to record the data shown in Figure 10.

Conclusions and Prospects

Gas-phase proteins should be viewed as tools to examine the interactions that are present in solution. They can provide information about the intrinsic intramolecular interactions and solvent interactions that cannot be obtained directly from solution studies. Thus, the impact of these studies will be to increase our general understanding of the interactions that drive biomolecules to fold and adopt particular conformations. With access to increasingly detailed information about the properties of proteins in the gas phase, and the prospect of performing more sophisticated simulations soon, this area will remain an exciting research frontier.

Many people have contributed to the work described here. The work would never have begun without suggestions and encouragement from a number of people in the mass spectrometry community. When we started, Melody Hsieh spent more than a year trying to get a MALDI source to work properly before David Clemmer came to the rescue, built an electrospray source, and obtained our first results. Konstantin Shelimov performed the studies of the unfolding and refolding processes. Robert Hudgins, Jürgen Woenckhaus, and Jim Fye were responsible for the hydration studies. The MD simulations were performed by Yi Mao in collaboration with Mark Ratner. Jiri Kolafa provided help and advice. The work was partially supported by the donors of the Petroleum Research Fund, administered by the American Chemical Society, and by the National Science Foundation.

References

(1) Whitehouse, C. M.; Dreyer, R. N.; Yamashuta, M.; Fenn, J. B. Electrospray Interface for Liquid Chromatographs and Mass Spectrometers. *Anal. Chem.* **1985**, *57*, 675−679.

(2) Karas, M.; Hillenkamp, F. Laser Desorption Ionization of Proteins with Molecular Masses Exceeding 10, 000 Daltons. *Anal. Chem.* **1988**, *60*, 2299−2301.

(3) See the Research News article Weighing DNA for Fast Genetic Diagnostics: Alper, J. *Science* **1998**, *279*, 2044.

(4) Wood, T. D.; Chorush, R. A.; Wampler, F. M.; Little, D. P.; O'Connor, P. B.; McLafferty, F. W. Gas-Phase Folding and Unfolding of Cytochrome c Cations. *Proc. Natl. Acad. Sci. U.S.A.* **1995**, *92*, 2451−2454.

(5) McLafferty, F. W.; Guan, Z.; Haupts, U.; Wood, T. D.; Kelleher, N. L. Gaseous Conformational Structures of Cytochrome *c*. *J. Am. Chem. Soc.* **1998**, *120*, 4732−4740.

(6) Cambell, S.; Rodgers, M. T.; Marzluff, E. M.; Beauchamp, J. L. Deuterium Exchange Reactions as a Probe of Biomolecule Structure. Fundamental Studies of Gas-Phase H/D Exchange Reactions of Protonated Glycine Oligomers with D_2O, CD_3OD, CD_3CO_2D, and ND_3. *J. Am. Chem. Soc.* **1995**, *117*, 12840−12854.

(7) Collings, B. A.; Douglas, D. J. Conformations of Gas-Phase Myoglobin Ions. *J. Am. Chem. Soc.* **1996**, *118*, 4488−4489.

(8) Cox, K. A.; Julian, R. K.; Cooks, R. G.; Kaiser, R. E. Conformer Selection of Protein Ions by Ion Mobility in a Triple Quadrupole Mass Spectrometer. *J. Am. Soc. Mass Spectrom.* **1994**, *5*, 127−136.

(9) Sullivan, P. A.; Axelsson, J.; Altman, S.; Qusit, A. P.; Sunqvist, B. U. R.; Reimann, C. T. Defect Formation on Surfaces Bombarded by Energetic Multiply-Charged Proteins: Implication for the Conformation of Gas-Phase Electrosprayed Ions. *J. Mass Spectrom.* **1995**, *7*, 329−341.

(10) Gross, D. S.; Schnier, Rodriguez-Cruz, S. E.; Fagerquist, C. K.; Williams, E. R. Conformations and Folding of Lysozyme Ions in Vacuo. *Proc. Natl. Acad. Sci. U.S.A.* **1996**, *93*, 3143−3148.

(11) Kaltashov, I. A.; Feneslau, C. Stability of Secondary Structure Elements in a Solvent Free Environment: The α-Helix. *Protein: Struct., Funct., Genet.* **1997**, *27*, 165−170.

(12) Hagen, D. F. Characterization of Isomeric Compounds by Gas and Plasma Chromatography. *Anal. Chem.* **1979**, *51*, 870−874. Karpas, Z.; Cohen, M. J.; Stimac, R. M.; Wernlund, R. F. Differentiating between Large Isomers and Derivation of Structural Information by Ion Mobility/Mass Spectrometry. *Int. J. Mass Spectrom. Ion Processes* **1986**, *83*, 163−175. Von Helden, G.; Hsu, M. T.; Kemper, P. R.; Bowers, M. T. Structures of Carbon Cluster Ions from 3 to 60 Atoms: Linears to Rings to Fullerenes. *J. Chem. Phys.* **1991**, *95*, 3835−3837.

(13) Wyttenbach, T.; Bushnell, J. E.; Bowers, M. T. Salt Bridge Structures in the Absence of Solvent? The Case for Oligoglycines. *J. Am. Chem. Soc.* **1998**, *120*, 5098−5103.

(14) Clemmer, D. E.; Hudgins, R. R.; Jarrold, M. F. Naked Protein Conformations: Cytochrome c in the Gas Phase. *J. Am. Chem. Soc.* **1995**, *117*, 10141−10142.
(15) Hoagland, C. S.; Valentine, S. J.; Sporieder, C. R.; Riley, J. P.; Clemmer, D. E. Three-Dimensional Ion Mobility/TOFMS Analysis of Electrosprayed Biomolecules. *Anal. Chem.* **1998**, *70*, 2236−2242.
(16) Fenn, J. B.; Mann, M.; Meng, C. K.; Wong, S. F.; Whitehouse, C. M. Electrospray Ionization Mass Spectrometry of Large Biomolecules. *Science* **1989**, *246*, 64−71.
(17) Chowdhury, S. K.; Katta, V, Chait, B. T. Probing Conformational Changes by Mass Spectrometry. *J. Am. Chem. Soc.* **1990**, *112*, 9012−9013.
(18) Mason, E. A.; McDaniel, E. W. *Transport Properties of Ions in Gases*; Wiley: New York, 1988.
(19) Mesleh, M. F.; Hunter, J. M.; Shvartsburg, A. A.; Schatz, G. C.; Jarrold, M. F. Structural Information from Ion Mobility Measurements: Effects of the Long-Range Potential. *J. Phys. Chem.* **1996**, *100*, 16082−16086.
(20) Shvartsburg, A. A.; Jarrold, M. F. An Exact Hard Spheres Scattering Model for the Mobilities of Polyatomic Ions. *Chem. Phys. Lett.* **1996**, *261*, 86−91.
(21) Shelimov, K. B.; Clemmer, D. E.; Hudgins, R. R.; Jarrold, M. F. Protein Structure in Vacuo: The Gas Phase Conformations of BPTI and Cytochrome c. *J. Am. Chem. Soc.* **1997**, *119*, 2240−2248.
(22) Bushnell, G. W.; Louie, G. V.; Brayer, G. D. High-Resolution Three-Dimensional Structure of Horse Heart Cytochrome *c*. *J. Mol. Biol.* **1990**, *214*, 585−595.
(23) Van Gunsteren, W. F.; Karplus, M. Protein Dynamics in Solution and in a Crystalline Environment: A Molecular Dynamics Study. *Biochemistry* **1982**, *21*, 2259−2274.
(24) Levitt, M.; Sharon, R. Accurate Simulation of Protein Dynamics in Solution. *Proc. Natl. Acad. Sci. U.S.A.* **1988**, *85*, 7557−7561.
(25) Shelimov, K. B.; Jarrold, M. F. Conformations, Unfolding, and Refolding of Apomyoglobin in Vacuum: An Activation Barrier for Gas-Phase Protein Folding. *J. Am. Chem. Soc.* **1997**, *119*, 2987−2994.
(26) Shelimov, K. B.; Jarrold, M. F. "Denaturation" and Refolding of Cytochrome *c* in Vacuo. *J. Am. Chem. Soc.* **1996**, *118*, 10313−10314.
(27) Hudgins, R. R.; Woenckhaus, J.; Jarrold, M. F. High-Resolution Ion Mobility Measurements for Gas-Phase Proteins: Correlation between Solution Phase and Gas Phase Conformations. *Int J. Mass Spectrom. Ion Processes* **1997**, *165/166*, 497−507.
(28) Mao, Y.; Woenckhaus, J.; Kolafa, J.; Ratner, M. A.; Jarrold, M. F. Thermal Unfolding of Gas-Phase Cytochrome *c*: Experiment and Molecular Dynamics Simulations. *J. Am. Chem. Soc.*, submitted for publication.
(29) Schnier, P. D.; Gross, D. S.; Williams, E. R. Electrostatic Forces and Dielectric Polarizability of Multiply Protonated Gas-Phase Cytochrome *c* Ions Probed by Ion/Molecule Chemistry. *J. Am. Chem. Soc.* **1995**, *117*, 6747−6757.
(30) Brooks, B. R.; Bruccoleri, R. E.; Olafson, B. D.; States, D. J.; Swaminathan, S.; Karplus, M. CHARMM: A program for Macromolecular Energy, Minimization, and Dynamics Calculations. *J. Comput. Chem.* **1983**, *4*, 187−215.
(31) Chowdhury, S. K.; Katta, V.; Chait, B. T. An Electrospray Ionization Mass Spectrometer with New Features. *Rapid Commun. Mass Spectrom.* **1990**, *4*, 81−87.
(32) Rodriguez-Cruz, S. E.; Klassen, J. S.; Williams, E. R. Hydration of Gas-Phase Gramicidin S $(M+2H)^{2+}$ Ions Formed by Electrospray: The Transition from Solution to Gas-Phase Structure. *J. Mass Spectrom.* **1997**, *8*, 565−568.
(33) Rupley, J. A.; Careri, G. Protein Hydration and Function. *Adv. Protein Chem.* **1991**, *41*, 37−172.
(34) Klassen, J. S.; Blades, A. T.; Kebarle, P. Determination of Ion−Molecule Equilibria Involving Ions Produced by Electrospray. Hydration of Protonated Amines, Diamines, and Some Small Peptides. *J. Phys. Chem.* **1995**, *99*, 15509−15517.
(35) Woenckhaus, J.; Hudgins, R. R.; Jarrold, M. F. Hydration of Gas-Phase Proteins: A Special Hydration Site on Gas-Phase BPTI. *J. Am. Chem. Soc.* **1997**, *119*, 9586−9587.
(36) Wlodawer, A.; Nachman, J.; Gilliland, G. L.; Gallagher, W.; Woodward, C. Structure of Form III Crystals of Bovine Pancreatic Trypsin Inhibitor. *J. Mol. Biol.* **1987**, *198*, 469−480.
(37) Otting, G.; Wüthrich, K. Studies of Protein Hydration in Aqueous Solution by Direct NMR Observation of Individual Protein-Bound Water Molecules. *J. Am. Chem. Soc.* **1989**, *111*, 1871−1875.
(38) Hermans, J.; Vacatello, M. Modelling Water-Protein Interactions in a Protein Crystal. *ACS Symp. Ser.* **1980**, *127*, 199−214.
(39) Fye, J. L.; Woenckhaus, J.; Jarrold, M. F. Hydration of Folded and Unfolded Gas-Phase Proteins: Saturation of Cytochrome *c* and Apomyoglobin. *J. Am. Chem. Soc.* **1998**, *120*, 1327−1328.
(40) Lee, B.; Richards, F. M. The Interpretation of Protein Structures: Estimation of Static Accesibility. *J. Mol. Biol.* **1971**, *55*, 379−400.
(41) Theorell, H.; Åkesson, Å. Studies on Cytochrome *c*: III. Titration Curves. *J. Am. Chem. Soc.* **1941**, *63*, 1818−1820.

AR960081X